residues. This structural model, experimentally based on side chain interactions alone, places residues in three-dimensional space on a single subunit (hence a 90° sector) of the homotetrameric K^+ channel and shows the extent of side chain exposure to the pore lumen or external vestibule. As a structural hypothesis, the model is necessarily crude, but its consistency with the localization of residues gathered by independent methods is encouraging (*7*, *21*, *25*, *26*). Although the model eschews explicit suggestions about backbone secondary conformation, the exposure pattern of the NH_2-terminal side of the P region (residues P0 to T9) is consistent with α-helical periodicity, as has been suggested in some models of the K^+ channel pore (*28*); the exposure pattern is inconsistent with a pore formed as an eight-stranded β barrel, as envisioned in other models (*3*, *29*).

With respect to ion selectivity mechanisms, these results allow us to draw two specific conclusions about a subset of P region residues. First, the residues projecting inward to line the narrow part of the pore begin beyond residue F3, at W4 or W5, not at P0. Second, it is now clear that among the P region's four aromatic side chains, three point toward the pore lumen: W4, W5, and Y15. Thus, the proposal (*7*, *30*) that K^+ in the pore is coordinated in a cage of π electrons, though in contention (*4*, *9*), remains viable.

REFERENCES AND NOTES

1. G. Yellen, *J. Gen. Physiol.* **84**, 157 (1984); J. Neyton and C. Miller, *ibid.* **92**, 569 (1988).
2. H. A. Hartmann *et al.*, *Science* **251**, 942 (1991).
3. G. Yellen, M. E. Jurman, T. Abramson, R. MacKinnon, *ibid.*, p. 939.
4. L. Heginbotham, Z. Lu, T. Abramson, R. MacKinnon, *Biophys. J.* **66**, 1061 (1994).
5. K. L. Choi, C. Mossman, J. Aube, G. Yellen, *Neuron* **10**, 533 (1993); P. A. Slesinger, Y. N. Jan, L. Y. Jan, *ibid.* **11**, 739 (1993); G. A. Lopez, Y. N. Jan, L. Y. Jan, *Nature* **367**, 179 (1994).
6. R. MacKinnon, *Nature* **350**, 232 (1991).
7. L. Heginbotham and R. MacKinnon, *Neuron* **8**, 483 (1992).
8. R. MacKinnon, R. W. Aldrich, A. W. Lee, *Science* **262**, 757 (1993).
9. C. Miller, *ibid.* **261**, 1692 (1993).
10. M. H. Akabas, D. A. Stauffer, M. Xu, A. Karlin, *ibid.* **258**, 307 (1992); M. H. Akabas, C. Kaufmann, T. A. Cook, P. Archdeacon, *J. Biol. Chem.* **269**, 14865 (1994); M. Xu and M. H. Akabas, *ibid.* **268**, 21505 (1993); M. H. Akabas, C. Kaufmann, P. Archdeacon, A. Karlin, *Neuron* **13**, 919 (1994); R. D. Zuhlke *et al.*, *Soc. Neurosci. Abstr.* **20**, 864 (1994).
11. R. S. Nyholm, *Proc. Chem. Soc.* **1961**, 273 (1961).
12. G. W. Liesegang, M. M. Farrow, F. A. Vazquez, N. Purdie, E. M. Eyring, *J. Am. Chem. Soc.* **99**, 3240 (1977).
13. O. S. Andersen, personal communication.
14. I. G. Dance, *Polyhedron* **5**, 1037 (1986).
15. L. Heginbotham, thesis, Harvard University (1993).
16. T. Hoshi, W. N. Zagotta, R. W. Aldrich, *Science* **250**, 533 (1990).
17. Potassium channels were expressed in *Xenopus* oocytes with *Shaker* H4 cDNA or Shaker-IR channels lacking residues 6 to 46 (*25*). Two independent clones of each mutation were characterized. RNA (0.2 to 0.5 ng) containing wild-type and cysteine-substituted P region was injected at an approximate ratio of 4:1. Injected oocytes were kept 2 to 3 days at 18°C until recording by two-electrode voltage clamp (Warner Instruments, OC-725B). The bath solution contained 96 mM $NaNO_3$, 2 mM KNO_3, 0.3 mM $Ca(NO_3)_2$, 1 mM $Mg(NO_3)_2$, and 10 mM Hepes-NaOH (pH 7.1). $AgNO_3$ stock solutions were stored in the dark before dilution in the experimental solution. Ag–AgCl electrodes were connected to the bath by means of fresh salt bridges containing 300 mM $NaNO_3$. Recording microelectrodes (0.2 to 0.8 megohms) were filled with 3 M KCl. Voltage commands and current acquisition were controlled with a Microstar DAP3200e acquisition board. Perfusion was controlled manually (exchange time ~10 s).
18. For brevity, we number the P region from P0 to P20, beginning with Shaker residue P430 and ending with P450. Abbreviations for the amino acid residues are as follows: A, Ala; D, Asp; F, Phe; G, Gly; K, Lys; M, Met; P, Pro; T, Thr; V, Val; W, Trp; and Y, Tyr.
19. L. Heginbotham, T. Abramson, R. MacKinnon, *Science* **258**, 1152 (1992).
20. M. de Biasi, J. A. Drewe, G. E. Kirsch, A. M. Brown, *Biophys. J.* **65**, 1235 (1993).
21. R. MacKinnon and G. Yellen, *Science* **250**, 276 (1990).
22. G. Yellen, D. Sodickson, T.-Y. Chen, M. E. Jurman, *Biophys. J.* **66**, 1068 (1994).
23. G. E. Kirsch *et al.*, *Neuron* **8**, 499 (1992); M. Taglialatela *et al.*, *Pfluegers Arch.* **423**, 104 (1993); E. Perozo, R. MacKinnon, F. Bezanilla, E. Stefani, *Neuron* **11**, 353 (1993).
24. R. MacKinnon, L. Heginbotham, T. Abramson, *Neuron* **5**, 767 (1990).
25. S. A. N. Goldstein, D. J. Pheasant, C. Miller, *ibid.* **12**, 1377 (1994).
26. P. Hidalgo and R. MacKinnon, *Science* **268**, 307 (1995).
27. L. M. Boland, M. E. Jurman, G. Yellen, *Biophys. J.* **66**, 694 (1994).
28. S. R. Durell and H. R. Guy, *ibid.* **62**, 238 (1992).
29. C. Miller, *Science* **252**, 1092 (1991); S. Bogusz, A. Boxer, D. D. Busath, *Protein Eng.* **5**, 295 (1992).
30. R. A. Kumpf and D. A. Dougherty, *Science* **261**, 1708 (1993).

31. We thank D. Naranjo for advice throughout these experiments and L. Heginbotham for critical reading of the manuscript. Supported in part by NIH grant GM-31768.

20 October 1994; accepted 29 December 1994

Revealing the Architecture of a K^+ Channel Pore Through Mutant Cycles with a Peptide Inhibitor

Patricia Hidalgo and Roderick MacKinnon

Thermodynamic mutant cycles provide a formalism for studying energetic coupling between amino acids on the interaction surface in a protein-protein complex. This approach was applied to the Shaker potassium channel and to a high-affinity peptide inhibitor (scorpion toxin) that binds to its pore entryway. The assignment of pairwise interactions defined the spatial arrangement of channel amino acids with respect to the known inhibitor structure. A strong constraint was placed on the Shaker channel pore-forming region by requiring its amino-terminal border to be 12 to 15 angstroms from the central axis. This method is directly applicable to sodium, calcium, and other ion channels where inhibitor or modulatory proteins bind with high affinity.

A remarkable property of K^+ channels is their ability to discriminate nearly perfectly between K^+ and Na^+ ions. Recent studies have identified several regions of K^+ channel proteins that mediate ion conduction (*1*, *2*). However, all evidence indicates that a short stretch of amino acids, the P (pore) region, is the sole determinant of K^+ selectivity (*3*). Scorpion toxins interact intimately with this region and can be used as a structural template to deduce the spatial organization of P region residues (*4*).

To assign the location of channel residues (Fig. 1A) with respect to the toxin structure (Fig. 1B), we applied a systematic analysis based on the following intuitive principle. If amino acid *a* on the toxin interacts with amino acid *b* on the channel, then the effect (on the toxin-channel equilibrium) of mutating residue *a* should depend on whether *b* is mutated. The cross influence of one mutation on the effect of another can be quantified using a thermodynamic cycle (Fig. 1C) to analyze experiments where *a* and *b* are mutated separately and then together. The arrows connecting each toxin-channel pair refer to mutation of either the toxin (horizontal arrows) or the channel (vertical arrows). Each arrow number represents the factor by which affinity changes along the direction of the arrow—that is, the equilibrium inhibition constant (K_i) of the toxin-channel pair at the tail of the arrow divided by the K_i value of the toxin-channel pair at the arrowhead. For example, $X1$ equals $K_i(\text{wt:wt})/K_i(\text{mut:wt})$, where wt:wt is the wild-type toxin–wild-type channel pair and mut:wt is the mutant toxin–wild-type channel pair (*5*). The affinity change in going from the wild-type toxin–wild-type channel interaction (Fig. 1C, upper left) to the mutant toxin–mutant channel interaction (Fig. 1C, lower right) must be the same regardless of the pathway taken; therefore, we have

$$X1 \cdot Y1 = X2 \cdot Y2 \qquad (1)$$

Dividing both sides of Eq. 1 by $X2 \cdot Y1$ leads

Department of Neurobiology, Harvard Medical School, Boston, MA 02115, USA.

to the coupling coefficient, Ω, defined as

$$\Omega = \frac{X1}{X2} = \frac{Y2}{Y1} = \frac{K_i(\text{wt:wt}) \cdot K_i(\text{mut:mut})}{K_i(\text{wt:mut}) \cdot K_i(\text{mut:wt})} \quad (2)$$

If the two mutated residues are independent of one another (that is, if they do not interact), then Ω will be unity. [If the toxin mutation (Fig. 1C) alters the affinity by the same factor for both the wild-type channel and the mutant channel, then $X1 = X2$.] If the residues interact and the mutations alter their interaction, then Ω will deviate from unity (6). In energetic terms, the degree of interaction, or coupling energy brought about by the double mutation, is given by $RT \ln(\Omega)$, where R is the gas constant and T is temperature. (All Ω values reported below are numbers greater than unity for ease of comparison of their magnitudes; if Ω is less than unity according to Eq. 2, then its reciprocal is given.) The application of mutant cycles to interactions between amino acids within a single protein has been described (7).

To exploit the electrostatic interactions known to mediate binding of the scorpion toxin agitoxin 2 (AgTx2) to the channel, we focused on acidic or basic residues (Fig. 1, A and B). A plot of Ω values (Fig. 1D and Table 1) shows the extent of interaction between charge-neutralizing mutations of the eight basic residues on the toxin (Fig. 1B) and charge-altering mutations at positions 422, 427, and 431 on the channel (Fig. 1A) (8). The value of Ω for the R24Q (toxin)–D431N (channel) pair is outstanding. Such a large value results because the R24Q mutation reduces toxin affinity for the wild-type channel to about one-thousandth of that of the wild-type toxin, but has little effect on toxin binding to a D431N mutant channel (Table 1). This outcome is expected if Arg^{24} and Asp^{431} form a strong and specific interaction with each other. Mutation of either residue alone disrupts the interaction so that subsequent mutation of the second residue has little further effect. This result contrasts with the independence of mutations observed for many other pairs. For example, the K427E channel mutation and the R24Q toxin mutation both have very large effects on affinity, but Ω is near unity (Table 1 and Fig. 1).

The value of Ω for the R24Q-D431N pair corresponds to a coupling energy of about 17 kJ mol^{-1}. Inspection of the Ω plot leads to the conclusion that the strong coupling between these two mutated residues must result from their local interaction and not from a global structural change of either the toxin or the channel. For example, if the R24Q mutation altered the toxin structure or caused the toxin to change its position in the binding site, then R24Q would in general be strongly coupled to many other channel mutations. Likewise, if the D431N mutation produced a global alteration of the channel structure, then strong coupling to multiple toxin mutations would be expected. Therefore, the singular large Ω at R24Q-D431N along the toxin and channel dimensions of the plot provides internal support for the structural integrity of both mutated molecules and reinforces the conclusion that Asp^{431} interacts locally with Arg^{24}.

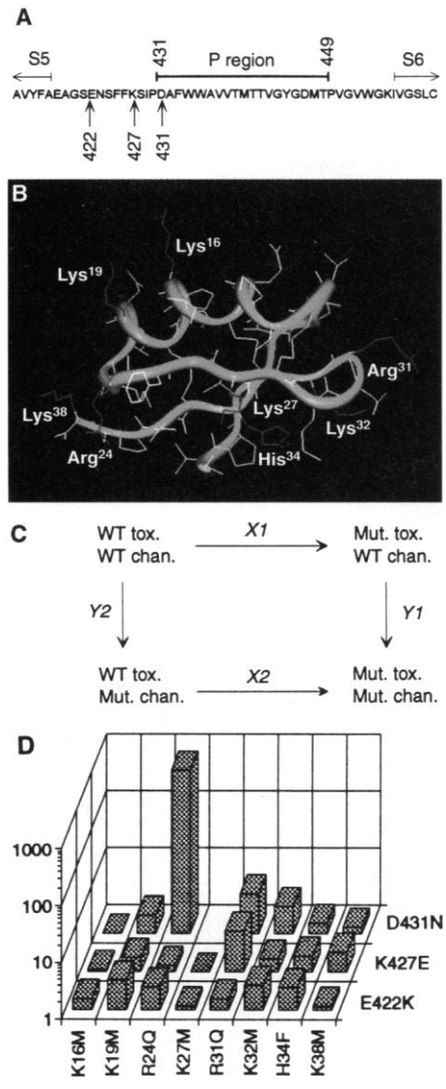

Fig. 1. Thermodynamic mutant cycles identify interactions between amino acids on the Shaker K^+ channel and AgTx2. (**A**) The partial sequence (*14*) of a Shaker K^+ channel subunit shows the S5-S6 linker and indicates the three toxin-interacting residues under study (arrows). The P region extends from residue 431 to residue 449. (**B**) The AgTx2 structure (*15*) is shown with a blue backbone ribbon; hydrogen atoms are omitted. The eight basic amino acids studied are shown in red, and the three disulfide bridges are shown in yellow. (**C**) Equilibrium inhibition constants (K_i) for the affinity of a wild-type toxin (WT tox.) and a mutant toxin (Mut. tox.) for a wild-type channel (WT chan.) and a mutant channel (Mut. chan.) define a thermodynamic cycle where *X1*, *X2*, *Y1*, and *Y2* represent change in affinity along the arrow. (**D**) Plot of Ω values calculated according to Eq. 2 for the paired mutations (*14*). Our inability to determine Ω for the K27M-D431N pair is compatible with their independence (Table 1).

Previous biophysical studies showed that Lys^{27} on an AgTx2 isoform interacts with ions in the K^+ channel pore (9). If Lys^{27} on AgTx2 is located centrally over the pore, then the strong interaction between Arg^{24} and Asp^{431} leads to the following prediction: Arg^{31}, located at the opposite side of the toxin from Arg^{24} (Fig. 2), should interact with Asp^{431} on a diagonally opposed channel subunit. This prediction is based on the expected fourfold symmetry of a Shaker K^+ channel (*10*). Arg^{31} and Arg^{24} are not exactly symmetric about Lys^{27}, and therefore their interactions with Asp^{431} residues on diagonal subunits should not be identical. Nevertheless, the strong interaction, which so tightly constrains the location of Asp^{431} on one subunit with respect to Arg^{24}, would place Asp^{431} on the diagonal subunit within a few angstroms of Arg^{31}. If Arg^{31} and Asp^{431} are indeed near each other in space, then coupling by means of a through-space electrostatic mechanism should be detectable on the Ω plot.

The value of Ω for the R31Q-D431N pair is 5.0 ± 0.6 (Fig. 1D and Table 1), which corresponds to a coupling energy of 4 kJ mol^{-1}. Although this interaction is weak, it is around the magnitude expected for through-space electrostatic coupling. For example, using Debye-Hückel theory, 4 kJ mol^{-1} translates into a 3 Å separation between two unit charges in a solution of 100 mM NaCl. To further test an electrostatic mechanism, we constructed a network of cycles by making multiple amino acid substitutions at these positions (Fig. 3A). A through-space electrostatic mecha-

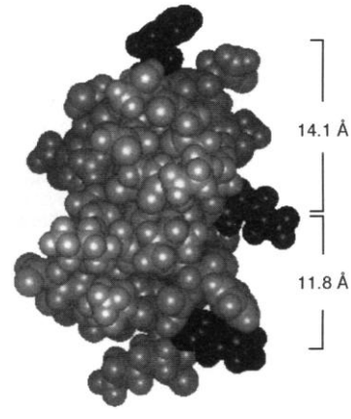

Fig. 2. A CPK model of AgTx2 shows (in dark) the side chains of Arg^{24} (bottom), Lys^{27} (middle), and Arg^{31} (top). The distances between the γ carbon atoms of Arg^{24} and Lys^{27} and between those of Arg^{31} and Lys^{27} are indicated.

nism predicts that mutations will show coupling only if the charge is altered on both the toxin and the channel. If the charge is conserved at the mutated site on either or both proteins, then no coupling ($\Omega = 1$) should be observed. The pattern of Ω values in the network fulfills this prediction. These results firmly establish the electrostatic nature of the interaction between residues at positions 31 (toxin) and 431 (channel). We therefore conclude that these residues are within a few angstroms of each other, as was hypothesized on the basis of purely geometric considerations.

Application of the cycle network analysis to characterize the strong interaction of the 24-431 pair confirms our earlier intuition that Arg^{24} and Asp^{431} interact through short-range molecular forces rather than through-space electrostatics (Fig. 3B). The value of Ω for all cycles is much greater than unity, independent of charge perturbation. Arg^{24} and Asp^{431} apparently come into intimate contact either sterically (with an electrostatic component) or, more likely, through the formation of an ionized hydrogen bond (salt bridge).

These data show that the distance separating residues Arg^{24} and Arg^{31} (about 25 Å) on opposite sides of a rigid toxin molecule is a measure of the spacing between Asp^{431} residues on diagonally opposed channel subunits. The relation between the Asp^{431} residues on four channel subunits with respect to the toxin is shown in Fig. 4. Asp^{431}, at the NH_2-terminal limit of the P region, is located 12 to 15 Å away from the

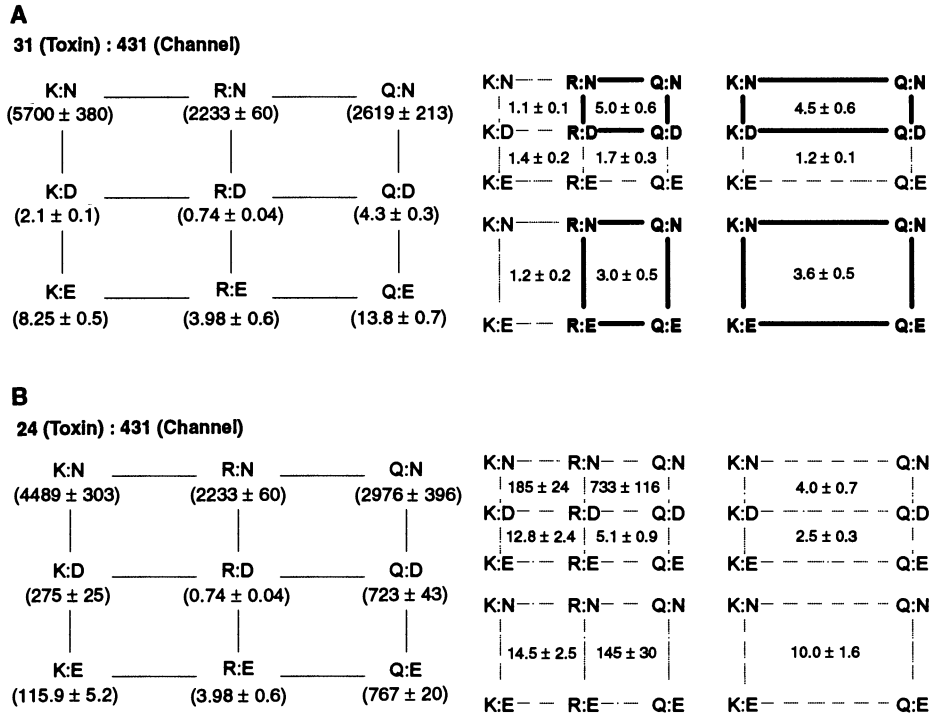

Fig. 3. Multiple amino acid substitutions involving a pair of residues allow the construction of a cycle network for studying the interaction between mutated residues. (**A**) The network contains nine toxin-channel pairs corresponding to all combinations of three residues at position 31 (toxin) with three residues at position 431 (channel). At each node, the amino acid (*14*) on the left refers to the toxin residue and that on the right refers to the channel residue. Inhibition constants (nanomolar, mean ± SEM of three to eight measurements) for each toxin-channel pair are shown in parentheses (left panel). The value of Ω for every possible cycle defined by the network is shown (right panel). Values of Ω for each cycle (reported as numbers greater than unity) were calculated according to Eq. 2 with K_i values that corresponded to the interaction pairs at the four corners of the cycle. Cycles with larger Ω values (3 to 5) are shown in bold. Note that Ω values for the four smallest cycles fully determine Ω values for the remaining five cycles. (**B**) The same analysis is shown for mutations at position 24 on the toxin and position 431 on the channel. In this case, coupling is observed for all cycles.

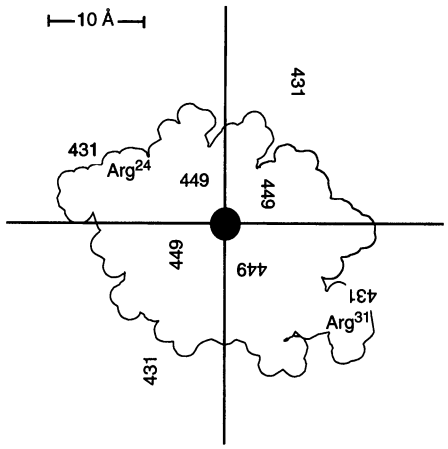

Fig. 4. Channel residue Asp^{431} is 12 to 15 Å from the central axis of the K^+ channel pore. The scalloped outline shows the shadow of AgTx2, oriented with Lys^{27} over the pore (black circle) at the interface between four subunits (defined by axes). The radial positions of channel residues 431 and 449 are shown. Residue 431 was placed near toxin residue Arg^{24} and then rotated by 90° about the central axis. Residue 449 was placed 5 Å from the center (*13*). The relative positions of residues 431 and 449 with respect to the subunit borders are arbitrary.

Table 1. Equilibrium inhibition constants (K_i, nM) and Ω values for pairs of channel and toxin mutants. The toxin mutations (left) were designed to neutralize basic amino acids. The channel mutations (top) altered the charge at three positions (422, 427, and 431) in the S5-S6 linker. Each K_i value is the mean ± SEM of three to eight separate measurements. NB refers to no inhibition at 2 μM (if the K27M and D431N mutations are independent, then the expected K_i for this pair is 1.7 mM). Values of Ω were calculated according to Eq. 2; for values less than unity, reciprocals are given for ease of comparison.

	WT	E422K		K427E		D431N	
	K_i	K_i	Ω	K_i	Ω	K_i	Ω
WT	0.74 ± 0.04	9.1 ± 0.7		0.007 ± 0.001		2233 ± 60	
K16M	1.42 ± 0.03	11.1 ± 0.8	1.6 ± 0.2	0.015 ± 0.001	1.1 ± 0.2	4092 ± 302	1 ± 0.1
K19M	2.7 ± 0.2	9.9 ± 0.5	3.4 ± 0.4	0.014 ± 0.001	1.8 ± 0.3	3791 ± 107	2.1 ± 0.2
R24Q	723 ± 43	3486 ± 264	2.6 ± 0.3	9.0 ± 0.7	1.3 ± 0.2	2976 ± 396	733 ± 116
K27M	575 ± 42	8400 ± 1000	1.2 ± 0.2	5.4 ± 0.2	1.0 ± 0.2	NB	–
R31Q	4.3 ± 0.3	32.7 ± 1.7	1.6 ± 0.2	0.21 ± 0.01	5.2 ± 0.9	2619 ± 213	5.0 ± 0.6
K32M	4.4 ± 0.3	20.0 ± 0.7	2.7 ± 0.2	0.025 ± 0.003	1.7 ± 0.3	4522 ± 223	3.0 ± 0.3
H34F	0.8 ± 0.1	24.9 ± 0.3	2.5 ± 0.5	0.004 ± 0.001	1.9 ± 0.6	3724 ± 174	1.5 ± 0.3
K38M	0.91 ± 0.03	9.1 ± 1.0	1.2 ± 0.2	0.019 ± 0.001	2.2 ± 0.3	2084 ± 160	1.3 ± 0.1

central axis (*11*). This conclusion is noteworthy for two reasons. First, this distance (12 to 15 Å) is nearly 10 times the radius of a K^+ channel selectivity filter, which has been estimated by functional measurements to be about 1.5 Å (*12*). The surprisingly distant radial location of Asp^{431} raises the possibility that a sizable segment of the P region could be oriented parallel rather than perpendicular to the plane of the membrane. Second, residue 449 at the COOH-terminal limit of the P region is known to be very close to the central axis (*13*). These findings lead us to propose that the P region forms a structure where side chains (or backbone carbonyls) from its COOH-terminal half line the narrow pore and interact with conducting ions. Results of experiments on ion selectivity are in agreement with this structural proposal (*3*).

Our results also explain why a Shaker K^+ channel with only a single subunit containing Asp^{431} (and three subunits containing Asn) is able to bind toxin with relatively high affinity (*10*). This property is a consequence of the strong interaction between Arg^{24} on the toxin and Asp^{431} on one subunit: As long as one subunit contains Asp^{431}, a permissive binding orientation exists. Asp^{431} on the diagonal subunit interacts only weakly (with Arg^{31}), and those on the two remaining subunits are located outside the toxin binding site (Fig. 4). Thermodynamic mutant cycles with a peptide inhibitor have placed a strong constraint on the structure of the P region of the K^+ channel. This approach will lead rapidly to a more complete picture of the surface structure of the K^+ channel pore.

REFERENCES AND NOTES

1. R. MacKinnon and G. Yellen, *Science* **250**, 276 (1990).
2. G. Yellen, M. E. Jurman, T. Abramson, R. MacKinnon, *ibid.* **251**, 939 (1991); H. A. Hartmann *et al.*, *ibid.*, p. 942; A. J. Yool and T. L. Schwarz, *Nature* **349**, 700 (1991); L. Y. Jan and Y. N. Jan, *ibid.* **371**, 119 (1994).
3. L. Heginbotham, T. Abramson, R. MacKinnon, *Science* **258**, 1152 (1992); M. De Biasi, G. E. Kirsch, J. A. Drewe, H. A. Hartmann, A. M. Brown, *Biophys. J.* **64**, A341 (1993); L. Heginbotham, Z. Lu, T. Abramson, R. MacKinnon, *ibid.* **66**, 1061 (1994).
4. M. Stocker and C. Miller, *Proc. Natl. Acad. Sci. U.S.A.* **91**, 9509 (1994).
5. The inhibition constant K_i is the equilibrium dissociation constant determined by measuring the functional blockade of channels. Toxin molecules bind to channels with 1:1 stoichiometry; the fraction of blocked channels is the same as the fraction of channels containing a bound toxin molecule.
6. It is possible (though unlikely) for mutations to alter an interaction between two residues in such a way that there is energetic compensation resulting in a Ω value of unity.
7. P. J. Carter, G. Winter, A. J. Wilkison, A. R. Fersht, *Cell* **38**, 835 (1984); L. Serrano, A. Horovitz, A. Boaz, M. Bycroft, A. R. Fersht, *Biochemistry* **29**, 9343 (1990); A. Horovitz and A. R. Fersht, *J. Mol. Biol.* **214**, 613 (1990).
8. All experiments were carried out with an inactivation-removed Shaker K^+ channel [T. Hoshi, W. N. Zagotta, R. W. Aldrich, *Science* **250**, 533 (1990)] expressed in *Xenopus laevis* oocytes. Oocytes were prepared and injected with RNA as described [R. MacKinnon, P. H. Reinhart, M. M. White, *Neuron* **1**, 997 (1988)]. K^+ currents were recorded with a two-electrode voltage clamp amplifier (Warner Instruments). Recording solution contained 95 mM NaCl, 2 mM KCl, 0.3 mM $CaCl_2$, 1 mM $MgCl_2$, and 5 mM Hepes buffer, pH 7.6. Currents were elicited with a 50-ms step to 0 mV every 5 to 25 s from a holding potential of −80 mV. Perfusion with toxin-free and toxin-containing solution was controlled with separate lines by means of computer-driven solenoids. Bovine serum albumin (50 μg/ml) was used to prevent nonspecific adherence of toxin to the perfusion lines. Current magnitudes ranged from 0.5 to 1.5 μA. The time course of the blockade of channels by toxin molecules was monitored to ensure that equilibrium inhibition was achieved and to confirm that the control current level was the same before addition and after removal of toxin. Three to eight experiments were performed on separate oocytes. Values of K_i were calculated according to the equation

$$K_i = \frac{[T](I/I_0)}{1 - (I/I_0)}$$

where I_0 is the control current level and I is the current in the presence of toxin concentration [T]. Channel mutants were produced and RNA transcription was carried out as described (*1*). Recombinant toxin was prepared as described [C. S. Park, S. F. Hausdorff, C. Miller, *Proc. Natl. Acad. Sci. U.S.A.* **88**, 2046 (1991); M. L. Garcia, M. Garcia-Calvo, P. Hidalgo, A. Lee, R. MacKinnon, *Biochemistry* **33**, 6834 (1994)]. An extinction coefficient of 8.6 mM^{-1} cm^{-1} at 235 nm was used to calculate toxin concentration. Mutants were produced in the toxin gene by means of polymerase chain reaction (PCR) mutagenesis and were confirmed by DNA sequencing across a Sal I–Hind III cassette containing the coding sequence.
9. C. S. Park and C. Miller, *Neuron* **9**, 307 (1992).
10. R. MacKinnon, *Nature* **350**, 232 (1991).
11. A range in the separation of Arg^{24} and Arg^{31} was determined by measuring the distance between the guanidinium carbon atoms in a superimposed set of 17 generated nuclear magnetic resonance structures. The distance of closest approach was 24 Å and that of greatest separation was 31 Å.
12. B. Hille, *Ionic Selectivity of Na^+ and K^+ Channels of Nerve Membranes* (Dekker, New York, 1975), pp. 255–323.
13. L. Heginbotham and R. MacKinnon, *Neuron* **8**, 483 (1992); M. P. Kavanaugh *et al.*, *ibid.*, p. 493; A. Gross and R. MacKinnon, in preparation.
14. Abbreviations for the amino acid residues are: A, Ala; C, Cys; D, Asp; E, Glu; F, Phe; G, Gly; H, His; I, Ile; K, Lys; L, Leu; M, Met; N, Asn; P, Pro; Q, Gln; R, Arg; S, Ser; T, Thr; V, Val; W, Trp; and Y, Tyr.
15. A. M. Krezel, C. Kasibhatla, P. Hidalgo, R. MacKinnon, G. Wagner, in preparation.

16. We thank B. Bean, A. Gross, Z. Lu, C. S. Park, R. Ranganathan, and K. Swartz for critical reviews of the manuscript. P.H. is a student from the Faculty of Sciences, University of Chile. This research was supported by NIH grant GM43949.

7 October 1994; accepted 6 January 1995